ADVANCED FUNCTIONAL MATERIALS

FULL PAPER

DOI: 10.1002/adfm.200601125

Surface-Enhanced Raman Scattering Using Microstructured Optical Fiber Substrates**

By *Adrian Amezcua-Correa*, *Jixin Yang*, *Chris E. Finlayson*, *Anna C. Peacock*, *John R. Hayes*, *Pier J. A. Sazio*,* *Jeremy J. Baumberg*, and *Steven M. Howdle*

Microstructured optical fibers (MOFs) represent a promising platform technology for fully integrated next generation surface enhanced Raman scattering (SERS) sensors and plasmonic devices. In this paper we demonstrate silver nanoparticle substrates for SERS detection within MOF templates with exceptional temporal and mechanical stability, using organometallic precursors and a high-pressure chemical deposition technique. These 3D substrates offer significant benefits over conventional planar detection geometries, with the long electromagnetic interaction lengths of the optical guided fiber modes exciting multiple plasmon resonances along the fiber. The large Raman response detected when analyte molecules are infiltrated within the structures can be directly related to the deposition profile of the nanoparticles within the MOFs via electrical characterization.

1. Introduction

The synthesis of metamaterials (periodically repeating, synthetic composite structures that are specifically designed to circumvent inconvenient bulk optical material properties) using micro/nanostructured scaffolds as templates is a powerful means to create 3D structures with appropriate nano-scale architecture.[1] The merit of a particular template structure, if it is to find wide practical application, will be defined by its robustness, temporal and mechanical stability, and its ability to be easily integrated within a range of systems. With these criteria in mind, optical fibers with internal capillary arrays present a number of attractive properties such as very large internal surface areas, high aspect ratios and outstanding mechanical properties, making them excellent lithography free, robust and inexpensive 3D templates for materials deposition.[2] The novelty and practicability of metal-functionalized MOF substrates opens up new possibilities for next generation of photonic devices and sensors. In this paper we report the fabrication of metal-dielectric composite MOFs using a high-pressure chemical deposition technique. The resulting structures are shown to serve as exceptional substrates for surface enhanced Raman spectroscopy (SERS).

MOFs are a special class of optical fiber whose guiding properties rely either on modified total internal reflection (TIR) or on the existence of photonic bandgaps.[3] In MOFs, the aperiodic or periodic arrangement of air holes can be tightly controlled during the fabrication process and, by choosing an appropriate structure, the spectral and temporal characteristics of the guided light can be carefully engineered.[4] A further advancement in the functionalization of MOFs is the inner modification and filling of their capillary holes. The deposition of useful materials inside the fiber voids has the potential to explore new directions in micro/nanomaterials technology and allow for long interaction lengths between guided modes of the fiber and the infiltrated materials. The incorporation of materials such as polymers, low-melting point metals, and gases has found use in complex optical in-fiber devices such as variable attenuators,[5] Mach-Zender interferometers[6] and Raman scattering gas cells.[7] However, filling the fiber capillaries with materials is extremely challenging since their pores have very high aspect ratios, and mass transport throughout their length is restricted.

More recently, high-pressure chemical deposition techniques have been developed for the inclusion of a wide range of technologically important materials such as silicon and germanium within MOF capillaries.[2] The empty capillary pores can be treated as microscale reaction chambers and by flowing a silver organometallic precursor solution through the fiber we have achieved the deposition of compact metal films along the fiber walls to create a new class of metallo-dielectric optical fiber de-

[*] Dr. P. J. A. Sazio, A. Amezcua-Correa, Dr. C. E. Finlayson, Dr. A. C. Peacock, J. R. Hayes
Optoelectronics Research Centre, University of Southampton
Southampton SO17 1BJ (UK)
E-mail: aac@orc.soton.ac.uk
Dr. J. Yang, Prof. S. M. Howdle
School of Chemistry, University of Nottingham
Nottingham NG7 2RD (UK)
Prof. J. J. Baumberg
School of Physics & Astronomy, University of Southampton
Southampton SO17 1BJ (UK)

[**] A.A.-C. and J.Y. contributed equally to this work. The authors acknowledge EPSRC for support under GR/S27771 and GR/S27764. A. Amezcua-Correa acknowledges the Mexican Council for Science and Technology for financial support. We thank R. Amezcua-Correa for assistance with mode profile simulations and J. R. Hyde for discussions on flow rate calculations. We also thank Mr M. Guyler, Mr R. Wilson, and Mr P. Fields for their technical assistance. S. M. Howdle is a Royal Society Wolfson Research Merit Award holder.

vices. Plasmonic[8] devices allow for the excitation of surface plasmon-polariton (SPP) modes, which are composite excitations combining oscillating electrons at optical frequencies with photons localized along the metal-dielectric interface. SPPs lead to a high concentration of the electromagnetic field at the surface boundary and this high localization of the field provides the electromagnetic contribution to surface enhanced Raman scattering. The ability of metallic nanostructures to mediate SERS effects is essential to achieve high sensitivity Raman spectroscopy, which can result in enhancements of more than 10^{14}, making detection practicable with possible applications right down to the single-molecule level.[9,10]

Since the discovery of SERS more than 30 years ago,[11] there have been tremendous developments in the surface sciences and nano-processing techniques that have permitted the fabrication of substrates with appropriate feature sizes. For example, using conventional semiconductor processing technologies, SERS templates have been produced via electron beam lithography,[12] focused ion beam patterning,[13] thermal evaporation[14] and chemical colloid reactions.[15] Although these substrates can provide high SERS signals, their fabrication can be costly, time consuming and is restricted to planar geometries that limit the interaction length over which plasmons can be excited along the device. Another important technology used in nanofabrication is "bottom-up" or self-assembly in which the metamaterial is fabricated by depositing the desired functional materials onto a 3D template.[1] Templates ranging from polymer nano-spheres,[16–18] to porous silicon[19] have been used to produce metallic SERS substrates. Bottom-up fabrication is simple and inexpensive but there are limitations on the creation of stable templates and the development of deposition methods inside high aspect ratio structures. Conventional planar SERS substrates do not have any optical guiding mechanism therefore the interaction area between the electromagnetic field and the analytes is restricted to the spot size of the laser beam. The fiber templating technique described here circumvents these limitations by combining the very long interaction length of optically guided modes with a template whose size and shape can be precisely controlled without lithography and is extremely robust, exhibiting a tensile strength greater than that of steel.[20] Although adding a metal nanoparticle coating into the holes of the MOF increases the optical loss due to the high absorption of metals at optical frequencies, centimeter long fibers enable the exploitation of plasmonic effects with acceptable optical loss. Previous attempts at deposition inside capillaries have exploited the immobilization of solution-based colloidal metal nanoparticles onto the silica walls.[21–23] However, this method does not provide control over the deposition thickness, the particle size is determined by the colloidal solution and, in order to achieve sufficient fluid flow, these devices have been restricted to internal dimensions of the order of 10 μm or greater.

This paper is organized as follows. Section 2 describes the fabrication process using the high pressure chemical deposition technique and presents examples of fibers coated under different deposition conditions. In Section 3, the fiber substrates are characterized using Raman measurements demonstrating SERS detection of a single molecular layer of benzenethiol. A qualitative explanation of the interaction between the optical modes and the metal nanoparticles is provided and the effects of the absorption loss is directly related to the SERS signal strength via two-terminal electrical measurements. Finally, in Section 4 we highlight the key features of the silver impregnated MOFs and outline their potential for use in remote sensing applications.

2. Fabrication of Metal-Dielectric MOFs

MOFs are typically fabricated by stacking and fusing capillary arrays into preforms a few centimeters in diameter and tens of centimeters in length, which are then drawn at high temperature.[24] The functionalization of the fibers is performed after the drawing process in a separate procedure. We employ an organic solvent under high pressure to deliver a silver precursor complex into the fiber holes. The high-pressure flow, which can be sustained due to the very high mechanical strength of optical fibers, overcomes mass-transport constraints within the extremely narrow fiber pores. This is followed by a simple thermal reduction of the precursor to form an annular deposition of silver nanoparticles inside the holes. The chosen precursor for the self-assembly of silver nanoparticles was Ag(hfac)(1,5-COD) (hfac = 1,1,1,5,5,5-hexafluoroacetylacetonato, COD = cyclo-octadiene) due to its high solubility in organic solvents (*n*-heptane), and also the desirable low decomposition temperature (200 °C) of this complex. The experimental chemicals, Ag(hfac)(1,5-COD) and *n*-heptane (HPLC grade), were purchased from Sigma-Aldrich and used as received.

Figure 1 shows a schematic of the experimental set-up used in the deposition work. Ag(hfac)(1,5-COD) is dissolved in *n*-heptane (typically up to 15 mg mL^{-1}) and the solution is flowed through the optical fiber at around 17 MPa by a high per-

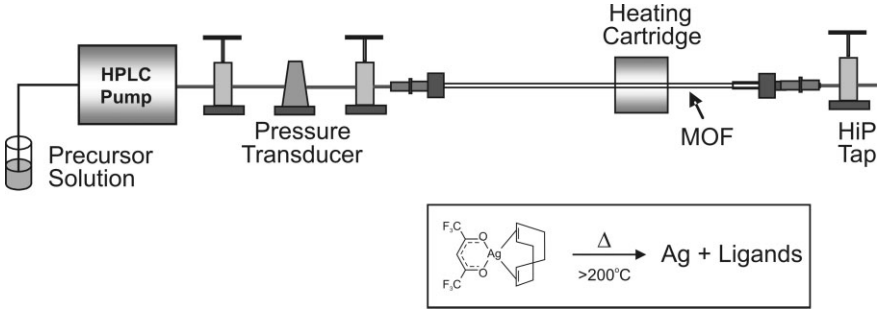

Figure 1. Schematic (not to scale) of the experimental set-up for the deposition of silver nanoparticles inside microstructured optical fibers. The decomposition of the organometallic precursor to form a compact silver film on the silica walls takes place within the heated area. The chemical structure of the organometallic silver precursor together with the decomposition process is shown in the inset.

formance liquid-chromatography pump. Due to the small volume contained in the fibers, the amount of precursor required for the deposition is tiny making the process safe even at the high pressures used in our experiment. The optical fiber is then fed through a 10 cm long heating cartridge with temperature PID control and HiP taps (High Pressure Equipment Company, USA) are used to control the precursor solution flow rate. As the precursor flows through the fiber, the furnace is heated up to 200 °C to initiate the deposition of silver nanoparticles. During the first few minutes of the process, metal begins to deposit onto the capillary walls. As the deposition time increases, the nanoparticles serve as nucleation points allowing the formation of thin granular films along the heated length. Run times for this process range between 0.5–3 hours depending on the desired deposition profile. After the deposition any decomposed ligands can be easily removed by the same solvent, leaving high purity silver grains inside the fiber. If required, supercritical CO_2 ($scCO_2$) can be flowed through the optical fiber to remove any trace of precursor (or any other unwanted by-products) left inside the holes. Figure 2 shows different silver coatings achieved by tuning the experimental parameters such as the deposition time, temperature, precursor

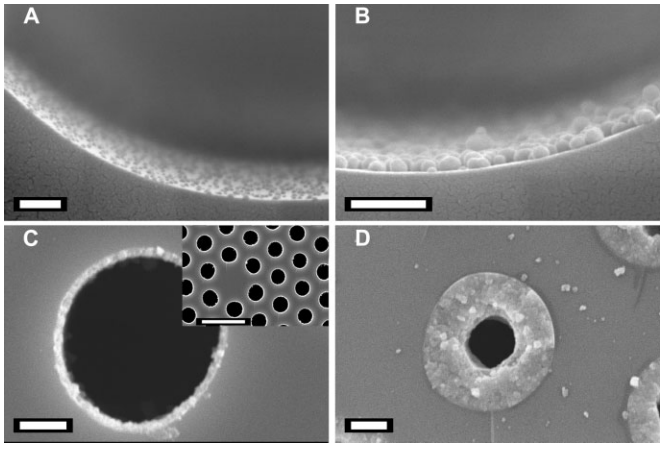

Figure 2. SEM images showing a range of silver deposition profiles obtained by tuning the experimental parameters. A) Deposition Time = 0.5 h with a precursor concentration of 5 mg mL^{-1}; 1 μm scale bar. B) Deposition Time = 0.5 h with a precursor concentration of 10 mg mL^{-1}; scale bar is 1 μm. C) Deposition Time = 2 h with a precursor concentration of 10 mg mL^{-1}; scale bars are 2 μm and 20 μm on the inset. D) Deposition Time = 3 h with a precursor concentration of 15 mg mL^{-1}; 2 μm scale bar.

concentration and flow rate. The silver nanoparticles diameter can be finely controlled from tens of nanometers to hundreds of nanometers, and the silver coating thickness up to a few microns. In all cases we observed a uniform filling of the holes across the fiber structure, as illustrated by the inset of Figure 2C. The longitudinal deposition profile is defined by the heater cartridge hot zone profile as a function of length as well as the precursor concentration, flow rate and deposition time. In our (non-optimized) deposition process, MOFs are typically impregnated over 15 cm with the central 5–6 cm having the most uniform filling. For our SERS experiments, the fiber samples were prepared in ~15 mm lengths so that a number of homogeneous SERS substrates could be obtained from the uniformly filled section, making the individual fabrication cost of the substrates low whilst the production rate is high.

3. Surface Enhanced Raman Characterization

The fiber substrates were tested for SERS activity using benzenethiol as the target molecule. Benzenethiol is a suitable molecule for investigating SERS due to its distinct Raman features, strong affinity for coinage-metal surfaces, and formation of self-assembled monolayers. All measurements were conducted using a conventional Renishaw Raman spectrometer with a 785 nm laser diode excitation source launched into a 20× microscope objective which produces a spot size of approximately 5 μm in diameter with 20 mW of optical power. In our experiments we investigated two fiber templates designed for modified TIR guidance; a triangular array containing 18 × 5 μm diameter air holes with a 20 μm silica core and a hexagonal array with 168 × 12 μm holes and a 15 μm core. The ~15 mm long sectioned samples were then treated with a drop of 1 mM benzenethiol solution in ethanol (purity > 98 % Aldrich and HPLC-grade Aldrich, respectively). After the solvent evaporated the fibers were rinsed then soaked in ethanol for 30 minutes. This procedure ensures that at most a monolayer of benzenethiol was present on the silver coating inside the fibers during the Raman measurements.

To illustrate the uniformity of the deposition over the cross-section of the structures, we have measured the SERS spectra at different positions across the cleaved face of a 168-hole fiber with a deposition profile and nanoparticle size distribution of the order of 100 nm,[25] as shown in Figure 2B. Under these launch conditions, the fiber modes that are excited are the lossy cladding modes that exist in our MOF templates because of the large silica fraction of the cladding (see Figs. 3A and 4B). The benzenethiol molecules that are absorbed onto the silver nanoparticles within the fiber couple to the SPP modes, thus releasing Raman scattered photons. The generated Raman photons are collected with the same objective lens used to focus the incident pump beam. Figure 3B shows the collected spectra corresponding to the positions marked on the SEM image of Figure 3A. A strong signal is observed in all cases and the main vibrational modes of the target molecule can be assigned as reported in the literature.[26] The detection of a monolayer of benzenethiol in the silver coated fibers is verified from the absence of the S-H molecular bond in the SERS spectra, as expected if all the molecules are attached directly to the silver surface.[27] Additionally, no Raman peaks were observed in a control fiber where 1 mM benzenethiol was impregnated into an empty (silica only) MOF of the same geometry and dimensions.

A significant feature of the spectra presented in Figure 3B is that the relative intensity is higher for the positions which are closer to the core of the fiber. To investigate this, we focused the incident beam onto the silica cores of the two different fiber templates to excite low loss guided modes. The 168-hole

ADVANCED FUNCTIONAL MATERIALS

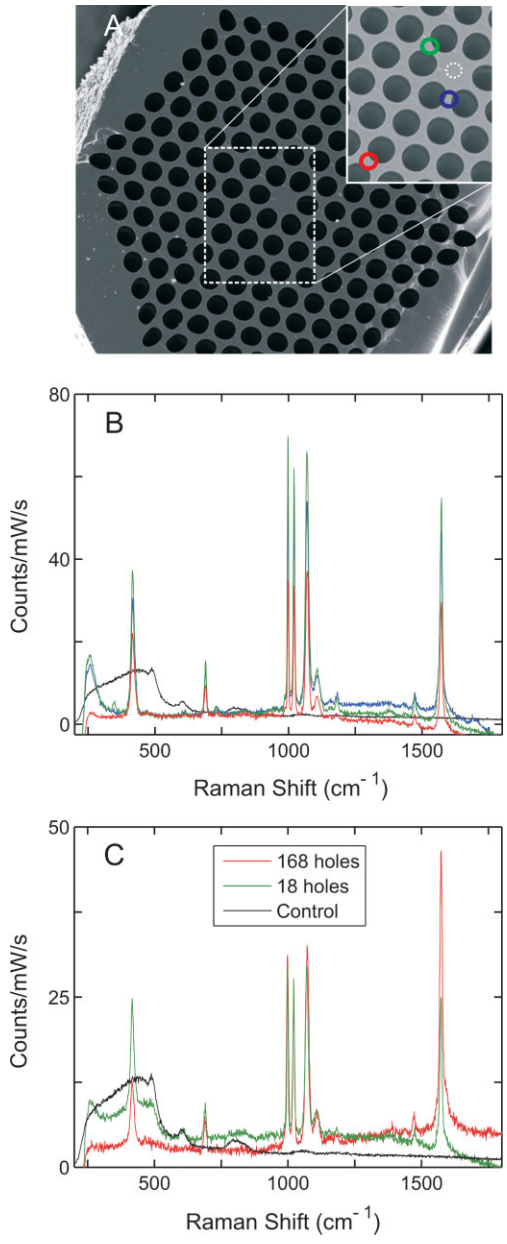

Figure 3. A) SEM image of the cleaved face of a low filling-fraction 168-hole MOF. A magnified view of the sampled area is shown in the inset. B) Color coded SERS spectra across the cleaved face of a 168-hole MOF corresponding to the colored positions marked on the micrograph inset. C) SERS spectra obtained from the 18 and 168-hole templates, with the incident excitation beam focused onto the silica cores as indicated by the dotted circle in the micrograph. In both spectra the Raman response from a control MOF with no silver filling is overlaid in black. To facilitate comparison, the SERS spectra have not been background corrected, but have all been shifted to have a baseline close to zero (counts/mW/s).

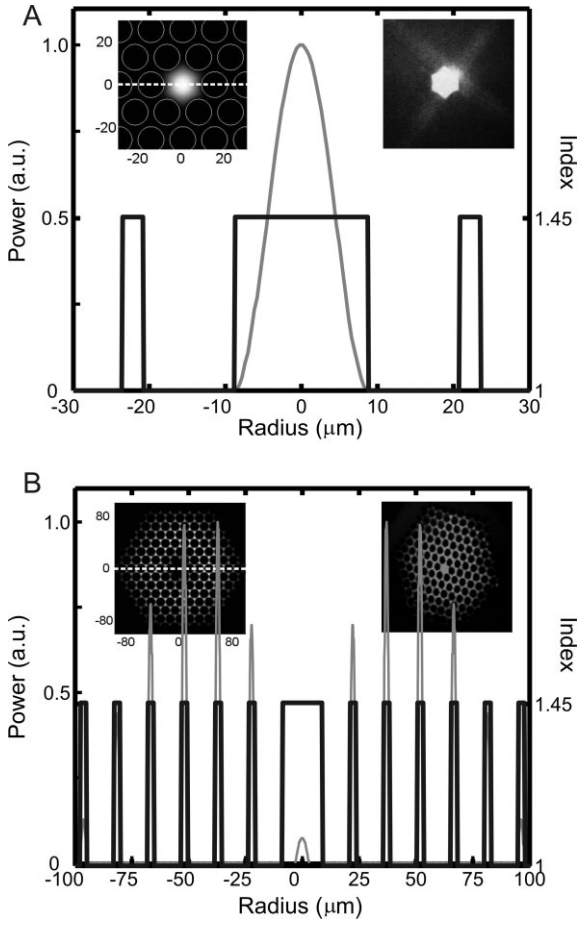

Figure 4. Calculated mode profile of the 168-hole MOF showing A) the fundamental guided mode and B) cladding filling mode at an excitation wavelength of 785 nm. The figures show the normalized power distribution across the silica MOF as a function of radial position, as indicated by the dotted lines across the 2D intensity plots shown in the top left insets. The top right insets show the distributed modes generated by launching a 632 nm laser into the control silica (i.e., no silver) fiber as imaged by an Electrophysics 7290A Vidicon camera.

MOF was the same as that used to obtain the data of Figure 3B, whereas 18-hole fiber corresponds to the deposition profile and nanoparticle size distribution shown in the inset of Figure 5D. Figure 3C shows the measured SERS spectra for the two samples, together with a control spectrum obtained from a fiber that has no silver impregnation, clearly illustrating the intense signal detectable in this configuration. Although the optical guided modes concentrate most of their energy in the core of the fiber, a small part of the energy is located in the air regions surrounding the core as evanescent fields which interact with the silver coating and excite surface plasmon resonances along the fiber length.[21] For our choice of pump wavelength, the fibers used in the experiments are multimode so that various SPP modes may be excited on a range of silver particles sizes. Using a full vectorial finite element method (FEM), we can calculate the profile and effective index of the fundamental guided mode for the 168-hole fiber. From this we find that the propagation confinement loss of an empty MOF structure is negligible, so that the losses can be estimated to be that of intrinsic silica at 785 nm, ~2 dB/km. The cut-back method was then used to experimentally measure the loss of a silver impregnated fiber with the same deposition profile and nanoparticle distribution as Figure 2B. We obtained an increased loss of ~2 dB cm^{-1}, as expected due to the high absorption of the metal. This indicates that despite the high optical loss, the

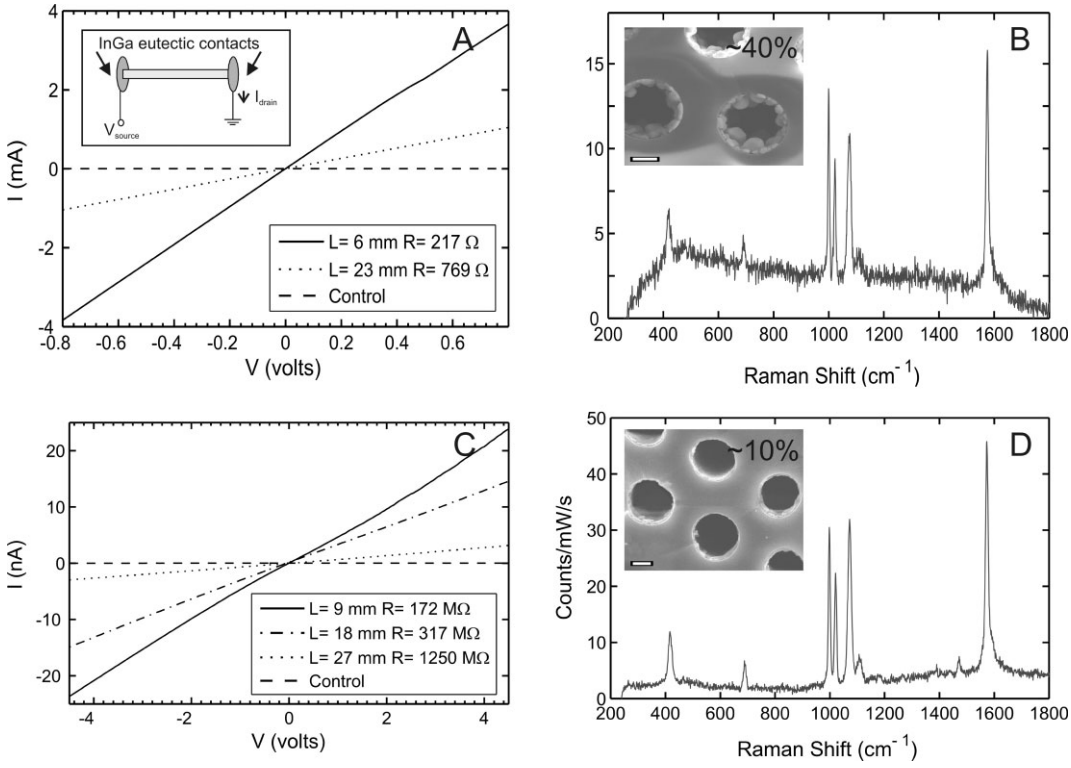

Figure 5. Current/voltage measurements on various lengths of two 18-hole silver filled MOFs with filling fractions of A) ~40% and C) ~10%. The samples had been cleaved at the ends and electrical contacts made with InGa eutectic (circuit diagram in top inset of A). The lengths corresponding to each curve are given in the insets with the calculated sample resistances based on an Ohmic model, together with control measurements on an unfilled silica MOF (dashed lines). B) and D) display the corresponding SERS response of the different filling fractions shown in the micrograph insets. Scale bars are 2 μm.

15 mm long fibers used in our experiments can provide a much larger interaction area compared to a planar substrate where the area is determined solely by the spot size of the pump laser. Furthermore, the mode guiding mechanism allows for averaging over the various particle sizes and spacing, thus moderating the effects of "hot spots". Owing to the unusual 3D geometry of the MOF SERS substrate the calculation of a precise enhancement factor, following the conventional methods presented in the literature, is nontrivial.[28] However, given a number of assumptions we can calculate a lower bound on the SERS enhancement factor. In particular we assume a single monolayer coverage, with a packing density of 6.8×10^{14} molecules cm^{-2},[29] over the entire 15 mm length and use the percentage of the fundamental guided mode in the air to estimate the power in the excitation field. Comparing our measurements to a standard Raman measurement on a bulk sample of pure benzenethiol, the resulting enhancement factor is estimated to be greater than 10^4, which compares favorably to enhancements reported elsewhere in the literature.

Using the FEM analysis we have calculated both the fundamental and higher order modes of an empty MOF. As shown in Figure 4A, the low loss fundamental guided mode in the core has only a small fraction of the overall power propagating in the air, resulting in relatively low excitation of nanoparticle plasmon resonances per unit (cross-sectional) area when silver is deposited inside the MOF. However, this is compensated by the long propagation length of the fundamental mode so that a large number of nanoparticle resonances can be excited adjacent to the core. Raman photons generated along the fiber are thus efficiently collected and guided by the high numerical aperture silica core and detected by the spectrometer. Conversely, in Figure 4B an example of a lossy cladding mode is shown which is far more delocalized across the periodic hole array and has a larger component propagating in the air with little or no power in the core. This results in substantially different behavior as the area of plasmonic interaction is larger, and many more silver nanoparticles will be excited per unit area; however, this increased excitation efficiency is offset by the lossy mode's shorter propagation distance, resulting in fewer plasmon resonances throughout the length of the fiber. In addition, the generated Raman photons are not well coupled and localized by the high NA core, resulting in low detection efficiency for this particular setup. In either scenario, the detected SERS signals are approximately equivalent in magnitude as can be seen by comparing the graphs of Figure 3B and C (showing the SERS response from various positions on the cladding and core, respectively), suggesting that the relative trade-offs of both modal excitation conditions roughly balance each other out.

Given the conflicting criteria of many nanoparticle plasmon excitations per unit area, versus long optical propagation distances and efficient Raman photon collection and detection, it

would at first appear that further improvements to our optical fiber based substrates will have to operate within these opposing constraints. However, the 168 and 18-hole MOFs used in these experiments are early stage designs and are thus relatively simple proof-of-principle structures with large, non-optimized feature sizes. Indeed, for the laser wavelength we are using in these experiments (785 nm), the large ~20 μm diameter core results in very few guided modes with any significant penetration of the optical power into the air holes. This suggests that in order to combine the desirable properties of large excitation areas with long propagation distances and efficient collection/detection, the ideal optical fiber characteristics would exhibit a large NA together with low loss guided modes that have a large optical component propagating in the voids. These criteria can be satisfied if we use a MOF design that has a small core diameter and a large air fraction honeycomb cladding[30] as this retains the high core-cladding refractive index contrast required for large NA, but at the same time requires the guided modes to propagate with a large amount of power in the air due to the small core size. We are currently investigating the SERS properties of such an optimized fiber design that has been impregnated with silver using the techniques reported here.

In addition to examining their optical properties, silver impregnated MOFs can also be electrically characterized to establish both the homogeneity and quantity of deposition, which is related to the observed SERS response. We performed electrical resistivity measurements on two 18-hole fibers with different silver filling fractions. The fibers were prepared by placing Indium-Gallium eutectic onto cleaved ends with the polymer coating removed. This provided a low resistance contact between the fiber and the probe station as illustrated in the inset of Figure 5A. Figure 5 shows the current versus voltage curves with silver filling fractions (defined as filled cross-sectional area of each pore) of approximately (A) 40 % and (C) 10 % for different sample lengths. For the fiber with a higher silver filling fraction, the resistance per millimeter of a 23 mm long sample increased slightly from 33.4 Ωmm^{-1} to 36.2 $\Omega\,mm^{-1}$ after re-cleaving to 6 mm (Fig. 5A), whereas for the lower silver filling fraction fiber the resistance per millimeter decreased from 46.30 $M\Omega\,mm^{-1}$ at 27 mm, to 17.61 $M\Omega\,mm^{-1}$ at 18 mm and 19.11 $M\Omega\,mm^{-1}$ at 9 mm lengths (Fig. 5C). This variation of the *I–V* behavior along the fiber length suggests that the deposition profile is not homogeneous for the low filling fraction sample; the particle density is sparse and so individual metal particle interactions may play an important role. We observed a strong correlation between the electrical resistance properties of optical fibers and the strength of their SERS response. This is illustrated in Figure 5B and D where the signal from the low filling fraction (high resistance) fiber is 3× higher than the (low resistance) sample with a high filling fraction, which can be attributed in part to the higher loss in the high filling fraction fiber. Other contributing effects will include increased scattering from the larger silver particles as well as plasmon resonance shifting and broadening. This very convenient electrical characterization method thus allows us to quickly scan through a number of samples to establish which deposition profiles are likely to provide a strong Raman response, and to obtain samples with reproducible SERS response.

An important consideration into the practicality of a SERS substrate is its temporal stability. Silver is regarded as having superior plasmonic properties to gold at visible wavelengths[31] due to the larger real (negative) part of its dielectric constant and its smaller imaginary (loss) component. However, as silver is prone to oxidation resulting in the strong suppression of surface plasmons, it has been largely neglected as a material for fabricating SERS substrates with high reproducibility. Despite this potential problem, the fiber structures we demonstrate here have been shown to generate efficient SERS signals months after they were fabricated, without special storage considerations, highlighting the temporal stability and mechanical robustness of the substrates. In addition, the high-pressure chemical deposition technique used to impregnate the MOFs is compatible with a wide range of solvents/precursors and therefore can be adapted for the deposition of other noble metals to achieve desirable optical and plasmonic properties. This flexibility allows us to exploit the unusual properties of solvents such as $scCO_2$, which combines low viscosity ($scCO_2$ has a viscosity in the range of 20–100 μPa s, whereas liquids at standard temperature and pressure have viscosities of approximately 500–1000 μPa s, and gases approximately 10 μPa s) with high diffusion rates, high density (close to 1 $g\,cm^{-3}$) and no surface tension. This makes $scCO_2$ an ideal choice for transporting reagents at high rates into extreme aspect ratio capillary geometries.[32] In addition, these properties are strongly pressure-dependent in the vicinity of the critical point, making $scCO_2$ a highly tunable solvent for a multitude of precursors. To date, we have successfully demonstrated uniform filling of a 2 μm hole MOF using $scCO_2$ as the solvent, with particle sizes ranging from >10 nm to 100 nm to give a granular layer thickness of the order 100 nm; the SERS response of these fibers is currently under investigation.

4. Conclusion

The high-pressure chemical deposition of metal nanoparticles within MOFs provides an effective method of creating in-fiber micro- and nano-scale structures that exploit co-operative photonic and plasmonic processes such as SERS. Specifically, the MOF design allows for cheap, fast, precisely controlled, highly reproducible and easily manufacturable template structures which to date has been a major limitation in the fabrication of SERS substrates.

The resulting metal-based MOFs offer many advantages over conventional planar SERS substrates such as: large interaction area between the optical wave and the analyte, highly extended electromagnetic interaction length, simple and quick electrical characterization, mechanical robustness and extreme aspect ratios that allows for the fabrication of sensors that can be used for chemical detection in microscale environments. In particular, MOF SERS substrates may open up new opportunities for remote Raman sensing. For example, a short section

at the end of a long (kilometer length) MOF can be modified with silver so that the low optical loss of the pure silica dielectric can be exploited to guide light to and from a remote location with the sensing capabilities of the metal modified tip.

In summary, we anticipate the fabrication of composite MOF structures that enhance the interaction between optical guided modes and internal metal nanostructures will prove a fruitful area for exploring plasmon engineering within optical waveguides.

5. Experimental

Sample Preparation: The chosen precursor for the self-assembly of silver nanoparticles was Ag(hfac)(1,5-COD) (hfac = 1,1,1,5,5,5-hexafluoroacetylacetonato, COD = cyclo-octadiene) due to its high solubility in organic solvents (*n*-heptane), and also the desirable low decomposition temperature (200 °C) of this complex. The experimental chemicals, Ag(hfac)(1,5-COD) and *n*-heptane (HPLC grade), were purchased from Sigma–Aldrich and used as received. Typical concentrations of the precursor solution range up to 15 mg mL^{-1}. For the deposition process, the optical fiber is fed through a 10 cm long heating cartridge with temperature PID control. HiP taps (High Pressure Equipment Company, USA) are used to control the precursor solution flow rate, ranging between 0.01–0.1 mL min^{-1}, depending on the fiber geometry. A LabAlliance Series III high performance liquid-chromatography pump is used to flow the precursor solution through the fiber at a total pressure of 17 MPa whilst the furnace is heated to 200 °C, thus initiating the deposition of silver nanoparticles. Typical run times for the process range between 0.5–3 hours depending on the desired deposition profile.

Loss Measurements: A 633 nm continuous wave (CW) 2 mW laser was launched using a 40 × objective into the cleaved end of a 4 cm long, 168 hole, silver impregnated MOF. The fiber axis was aligned using *xyz* micrometer drive stages. Measurement of the output power from the fiber end was performed using a Newport 2832C power meter with a silicon detector. We used a cut-back method to decouple other loss mechanisms such as Fresnel reflection from the measurement. By recleaving the fiber to 3.1 cm and then 1.3 cm, the loss was measured to be ~2 dB cm^{-1}. Transmission experiments performed at 785 nm also yielded a similar loss figure of ~2 dB cm^{-1}.

Received: November 22, 2006
Revised: February 22, 2007
Published online: July 24, 2007

[1] J. J. Baumberg, *Nat. Mater.* **2006**, *5*, 2.
[2] P. J. A. Sazio, A. Amezcua-Correa, C. E. Finlayson, J. R. Hayes, T. J. Scheidemantel, N. F. Baril, B. R. Jackson, D. J. Won, F. Zhang, E. R. Margine, V. Gopalan, V. H. Crespi, J. V. Badding, *Science* **2006**, *311*, 1583.
[3] P. S. J. Russell, *Science* **2003**, *299*, 358.
[4] J. C. Knight, *Nature* **2003**, *424*, 847.
[5] C. Kerbage, A. Hale, A. Yablon, R. S. Windeler, B. J. Eggleton, *Appl. Phys. Lett.* **2001**, *79*, 3191.
[6] M. Fokine, L. E. Nilsson, A. Claesson, D. Berlemont, L. Kjellberg, L. Krummenacher, W. Margulis, *Opt. Lett.* **2002**, *27*, 1643.
[7] F. Benabid, J. C. Knight, G. Antonopoulos, P. S. J. Russell, *Science* **2002**, *298*, 399.
[8] W. L. Barnes, A. Dereux, T. W. Ebbesen, *Nature* **2003**, *424*, 824.
[9] S. M. Nie, S. R. Emery, *Science* **1997**, *275*, 1102.
[10] K. Kneipp, Y. Wang, H. Kneipp, L. T. Perelman, I. Itzkan, R. Dasari, M. S. Feld, *Phys. Rev. Lett.* **1997**, *78*, 1667.
[11] M. Fleischmann, P. Hendra, A. McQuillan, *Chem. Phys. Lett.* **1974**, *26*, 163.
[12] L. Gunnarsson, E. J. Bjerneld, H. Xu, S. Petronis, B. Kasemo, M. Kall, *Appl. Phys. Lett.* **2001**, *78*, 802.
[13] A. G. Brolo, E. Arctander, R. Gordon, B. Leathem, K. L. Kavanagh, *Nano Lett.* **2004**, *4*, 2015.
[14] T. Vo-Dinh, *Sens. Actuators B* **1995**, *29*, 183.
[15] E. J. Bjerneld, F. Svedberg, M. Kall, *Nano Lett.* **2003**, *3*, 593.
[16] J. C. Hulteen, R. P. Vanduyne, *J. Vac. Sci. Technol. A* **1995**, *13*, 1553.
[17] S. Coyle, M. C. Netti, J. J. Baumberg, M. A. Ghanem, P. R. Birkin, P. N. Bartlett, D. M. Whittaker, *Phys. Rev. Lett.* **2001**, *87*, 176 801.
[18] J. J. Baumberg, T. A. Kelf, Y. Sugawara, S. Cintra, M. E. Abdelsalam, P. N. Bartlett, A. E. Russell, *Nano Lett.* **2005**, *5*, 2262.
[19] S. Chan, S. Kwon, T. W. Koo, L. P. Lee, A. A. Berlin, *Adv. Mater.* **2003**, *15*, 1595.
[20] C. R. Kurkjian, J. T. Krause, M. J. Matthewson, *J. Lightwave. Technol.* **1989**, *7*, 1360.
[21] W. Q. Xu, S. P. Xu, Z. C. Lu, L. Chen, B. Zhao, Y. Ozaki, *Appl. Spectrosc.* **2004**, *58*, 414.
[22] H. Yan, C. Gu, C. Yang, J. Liu, G. Jin, J. Zhang, L. Hou, Y. Yao, *Appl. Phys. Lett.* **2006**, *89*, 204 101.
[23] H. K. Park, H. B. Lee, K. Kim, *Appl. Spectrosc.* **2007**, *61*, 19.
[24] T. M. Monro, D. J. Richardson, *CR. Phys.* **2003**, *4*, 175.
[25] M. Moskovits, *J. Raman Spectrosc.* **2005**, *36*, 485.
[26] S. W. Han, S. J. Lee, K. Kim, *Langmuir* **2001**, *17*, 6981.
[27] W. K. Yi, C. W. Park, M. S. Kim, K. Kim, *Bull. Korean Chem. Soc.* **1987**, *8*, 291.
[28] Z.-Q. Tian, B. Ren, D.-Y. Wu, *J. Phys. Chem. B* **2002**, *106*, 9463.
[29] C. L. Haynes, R. P. Van Duyne, *J. Phys. Chem. B* **2003**, *107*, 7426.
[30] J. H. Lee, W. Belardi, K. Furusawa, P. Petropoulos, Z. Yusoff, T. M. Monro, D. J. Richardson, *IEEE Photonic Tech. L* **2003**, *15*, 440.
[31] P. B. Johnson, R. W. Christy, *Phys. Rev. B* **1972**, *6*, 4370.
[32] H. M. Woods, M. M. C. G. Silva, C. Nouvel, K. M. Shakesheff, S. M. Howdle, *J. Mater. Chem.* **2004**, *14*, 1663.